ISSN 1063-7745, Crystallography Reports, 2018, Vol. 63, No. 5, pp. 849–858. © Pleiades Publishing, Inc., 2018.
Original Russian Text © A.V. Mandrykina, D.N. Khmelenin, N.N. Kolobylina, A.L. Vasil'ev, T.N. Smekalova, N.F. Fedoseev, E.Yu. Tereschenko, O.A. Alekseeva, E.B. Yatsishina, 2018, published in Kristallografiya, 2018, Vol. 63, No. 5, pp. 832–841.

## CRYSTALLOGRAPHIC METHODS IN HUMANITARIAN SCIENCES

# Study of the Ancient Crimean Ceramics by Electron Microscopy Methods

**A. V. Mandrykina[a], D. N. Khmelenin[b], N. N. Kolobylina[a], A. L. Vasil'ev[a,b], T. N. Smekalova[a,c], N. F. Fedoseev[d], E. Yu. Tereschenko[a,b,*], O. A. Alekseeva[b], and E. B. Yatsishina[a]**

[a] *National Research Centre "Kurchatov Institute," Moscow, 123182 Russia*

[b] *Shubnikov Institute of Crystallography, Federal Scientific Research Centre "Crystallography and Photonics," Russian Academy of Sciences, Moscow, 119333 Russia*

[c] *Vernadsky Crimean Federal University, Simferopol, 295051 Russia*

[d] *Institute of Archaeology of Crimea, Russian Academy of Sciences, Simferopol, 295007 Russia*

**e-mail: helena.tereschenko@gmail.com*

Received March 30, 2018

**Abstract**—Fragments of ancient amphorae and tiles dated to the IVth to IInd centuries BC, which were found on the Crimean peninsula, have been investigated by methods of scanning and transmission/scanning electron microscopy, combined with energy-dispersive X-ray microanalysis. The revealed differences in the compositions of the clay core and inclusions (leaners) are associated with the differences in the periods of time when items were made and the sites of their origin.

**DOI:** 10.1134/S106377451805019X

## INTRODUCTION

Among archaeological artifacts, ceramic cultural heritage sites are much more widespread than those made of other materials. The reason is that ceramic products are more resistant against corrosion and are preserved much better than metal, wooden, and other artifacts. At the same time, ceramic products are a very important source of information about the material culture of ancient people, history of trade relationships, and development of handicrafts [1–9].

The study of ceramics is especially important for Crimea, which is at the frontier between the ancient civilization and the world of local tribes: archaeologists find numerous ceramic artifacts of ancient epoch in excavations of both ancient Greek and "barbarian" settlements and burials. These artifacts often have manufacturer's marks, which are the main dating material and source of information about the trade and cultural relationships between the ancient Greek centers of the Northern Black Sea region, the Mediterranean, and local tribes. At the same time, there are numerous ceramic finds with lost or absent marks, for which the production place and time must be determined.

The studies of the ceramic artifacts from Crimea have a long history. Since the 1950s, investigations in this field were aimed at developing a unified classification and constructing a commodity exchange network between the towns and states of the Black Sea region [10]. A conventional approach to determining the mineral composition of ceramics implies petrographic analysis on thin cuts or laps. A significant contribution to the study of amphora containers was made by Shcheglov and Selivanova, who used petrography to identify the clay mass of the amphoras of late Classical and early Hellenistic times from different centers in the Black Sea region, including Tauric Chersonesus [11]. Petrographic analysis of laps was supplemented in [12–15] with elemental analysis, electron microscopy, and microanalysis of elemental composition. The data obtained facilitated classification of the Pontic amphorae dated to the I BC–early III AD period and made it possible to select the main pottery centers. The mineralogical and petrographic studies of gray-clay dishes manufactured in the first centuries AD, combined with thermal, vacuum- decryptometric, and chromatographic analyses, gave grounds to conclude that the items under study were imported from the early Alanian pottery making centers of the Vladikavkaz plain and adjacent territories [16].

The worthiness and importance of studying ceramic items when analyzing the ancient trade relations was substantiated in [10]. At the same time, precise modern physical analytical methods have not been widely applied in Russian archaeology, although several successful studies were carried out by a research team from the St. Petersburg State Pedagogical University [17–19].

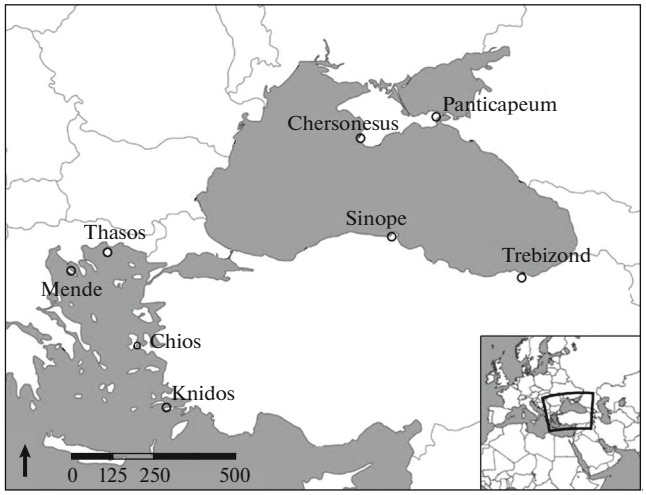


**Fig. 1.** Map with indicated origin of the samples studied.

The application efficiency of scanning electron microscopy (SEM), transmission electron microscopy (TEM), and energy-dispersive X-ray spectroscopy (EDXS) microanalysis (in the study of ceramics was considered in reviews [20–22]. It was noted that a joint use of SEM and EDXS makes it possible to determine the elemental composition of clays forming the matrix (base) of a ceramic product and select mineral microinclusions in this base, such as quartz, pyroxene, or volcanic glass. With these data at hand, one can carry out a more exact quantitative analysis of the base. In some cases [23, 24], when carrying out a phase analysis of the clay base (generally, using electron diffraction (ED), high-resolution transmission electron microscopy (HRTEM), or X-ray diffraction (XRD)), the ceramic annealing temperature was determined. In particular, application of SEM and EDXS in [24] revealed the ceramics to be multilayer composites (illite layers in most cases), not completely crystallized and having a wavy morphology. Proceeding from the phase state of the ceramics, its annealing temperature was found to be no higher than 850°C. No less interesting data were obtained using TEM and EDXS [25].

In this paper, we report the results of electron microscopy (EM) studies (using SEM, TEM, scanning transmission electron microscopy (STEM) in combination with EDXS) and XRD analysis of ceramic items dated to I–IV BC from the museum collections of the Crimea peninsula, based on the materials of long-term excavations.

## MATERIALS

The samples of study were as follows: (I) Bosporus tile (IV BC), (II) Sinopean amphora (III BC), (III) Sinopean amphora (II–I BC), (IV) Thasian amphora (III BC), (V) Thasian amphora (IV BC), (VI) Chersonesean amphora (IV BC), (VII) "Colchian" (Trebizond) amphora (II–I BC), (VIII) Chios amphora (IV BC), (IX) Knidos amphora (III BC), (X) Mendean amphora (IV BC), (XI) Bosporus tile (second half IV BC), and (XII) Bosporus tile (IV BC). The map of sample origin centers is presented in Fig. 1.

## METHODS OF STUDY

In the first stage, samples of ceramic artifacts were investigated by optical microscopy (OM). To this end, the samples were ground from one side using diamond disks. Images were obtained with an optical binocular microscope LeicaIC80 HD (Leica). OM images were processed applying the ImageJ software (NIST).

The EM study of the samples was performed on a Versa 3D double-beam scanning electron microscope with a focused ion beam (FIB) (FEI), equipped with an EDXS system (EDAX), in the natural-environment mode (40–4000 Pa), which made it possible to study nonconducting ceramic samples at an accelerating voltage of 20 kV. More detailed investigations were performed by the TEM and STEM methods using a wide-angle annular dark-field detector in an OSIRIS microscope (FEI), equipped with an Super-X EDXS (Bruker), at an accelerating voltage of 200 kV. Micrographs were processed using the DigitalMicrograph (Gatan), TIA (FEI,), and Esprit (Bruker) software packages. The local chemical composition of the clay base was determined on regions without any visible inclusions in order to minimize their influence on the calculation of concentrations. Note that the determination of the elemental composition by the EDX method was performed in the semiquantitative mode without mineral reference calibration; therefore, the error in determining the content of light elements (O and C) may be rather large.

## PREPARATION OF SAMPLES FOR STUDIES

Laps of ceramic samples were prepared for optical and SEM/EDXS studies.

Samples for TEM were prepared by grinding ceramic fragments in a mortar with subsequent ultrasonic dispersion in acetone and deposition on EM copper grids with a carbon substrate.

A group of black inclusions was prepared for analysis by the HRTEM and STEM/EDXS using an FIB on scanning microscopes Versa 3D (FEI) and Scios (FEI), according to the standard technique [26].

## RESULTS AND DISCUSSION

### *OM Studies and Comparison with SEM/EDX Data*

OM images of laps made on samples I–XII are presented in Fig. 2. Primarily, we considered the first feature of the ceramic samples: clay base color, which

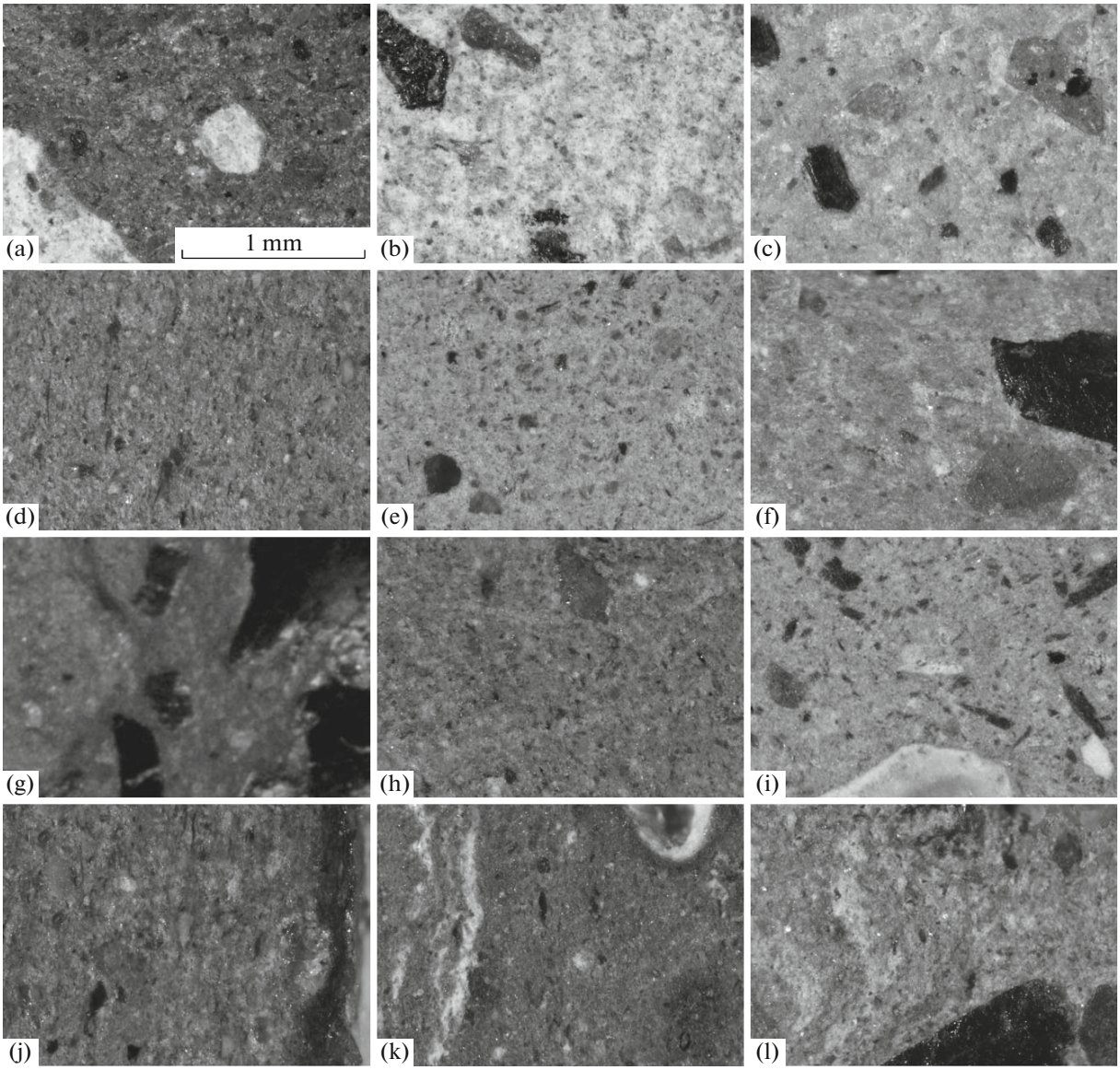


**Fig. 2.** OM images of laps of all samples, from (a) I to (l) XII.

varied from light beige (Fig. 2b) to dark brown (Fig. 2k). Then we analyzed the second feature: the presence of inclusions, which differed in size and color. The clay base color depends on the chemical composition and structure; having analyzed the latter, one can determine the source of raw material. The sizes of inclusions and their existence in the crystalline state may be related to the type of nonplastic material used in a specific workshop. These data may indicate the place of artifact production.

### *Study of the Clay Base. OM Results As Compared with SEM/EDXS Data*

A comparison of the clay bases of Thasian amphoras (i.e., the artifacts found in the same geographic region)—samples IV and V, fabricated in the III and IV centuries BC, respectively—shows that they have relatively close colors and similar character of dispersivity. The Bosporus tiles (samples I, XI and XII) are also characterized by similar clay bases.

The clay core is an aluminosilicate matrix with a relatively low content of Ca, Fe, Mg, C, K, and Na, i.e., the elements characteristic of clay minerals [27]. The SEM/EDXS data on the elemental composition of clay bases are listed in Table 1 for comparative analysis. One can see that the Ca and Fe contents change significantly: from 1 to 14.5 wt % and from 3.8 to 9.4 wt %, respectively. No direct relationship was revealed between the iron content and clay base color. In particular, the iron content in the samples having similar colors is not the same within allowable error.

**Table 1.** Comparative analysis of the elemental composition (wt %) of the clay base, determined by the EDX method in SEM and STEM

| Sample | I | | II | | III | | IV | | V | | VI | |
|---|---|---|---|---|---|---|---|---|---|---|---|---|
| Elements | SEM | STEM | SEM | STEM | SEM | STEM | SEM | STEM | SEM | STEM | SEM | STEM |
| O | 41.1 | 36.9 | 42.7 | 43 | 46.4 | 47.1 | 46.9 | 45.2 | 40.9 | 41.1 | 44.6 | 44.5 |
| Si | 22 | 36.3 | 23.5 | 25.9 | 25.6 | 24.0 | 17.9 | 18.3 | 21.9 | 25.9 | 22.8 | 21.5 |
| Ca | 8.5 | – | 9.3 | 9.8 | 2.4 | 1.2 | 5.7 | <1 | 8.9 | 9.6 | 9.6 | 14.4 |
| Al | 8.1 | 11.7 | 9.2 | 14.1 | 10.8 | 19.9 | 9.6 | 9.6 | 9.1 | 13.3 | 10.9 | 18.4 |
| Fe | 9.4 | – | 6.2 | 2.2 | 5.4 | 3.9 | 4.9 | 8.5 | 5.2 | 5.2 | 5.9 | 1.2 |
| Mg | 1.4 | – | 2.3 | 1.2 | 1.2 | 1.9 | 2.9 | 10.2 | 2 | 2.4 | 1 | – |
| C | 5.2 | – | 2.3 | – | 4.7 | – | 8.2 | – | 7.1 | – | 1.3 | – |
| K | 2.2 | 12.1 | 2 | 1.8 | 1.7 | 1.1 | 2.1 | 6.1 | 3.3 | 1.8 | 2.6 | – |
| Na | <1 | – | 1.4 | 1.6 | 1.3 | – | 1.3 | <1 | <1 | <1 | <1 | – |
| Sample | VII | | VIII | | IX | | X | | XI | | XII | |
| Elements | SEM | STEM | SEM | STEM | SEM | STEM | SEM | STEM | SEM | STEM | SEM | STEM |
| O | 48.3 | 48 | 42.8 | 35.4 | 44.7 | 47.8 | 42.9 | 46.6 | 45.6 | 40.3 | 44 | 44.9 |
| Si | 30.4 | 27.5 | 17.8 | 23.5 | 23.9 | 23.5 | 15.7 | 25.8 | 28.8 | 26.7 | 21.6 | 23.9 |
| Ca | 1.1 | 1.1 | 8 | 20.1 | 4.4 | 4.4 | 14.5 | <1 | 4.9 | 7.2 | 9.5 | 9.4 |
| Al | 9.2 | 11.6 | 8 | 12.6 | 9.1 | 13.7 | 7 | 23.6 | 8.4 | 15.6 | 8.3 | 13.4 |
| Fe | 6.3 | 8.6 | 3.8 | 1.9 | 4.7 | 3.2 | 5.4 | 2 | 6.6 | 3.4 | 7.1 | 3.0 |
| Mg | 1 | 1.6 | 2.2 | 1.3 | 3.1 | 2.8 | 3.3 | – | 1.3 | 1.8 | 1.6 | 1.7 |
| C | – | – | 12.2 | – | 6.3 | – | 7.7 | – | – | – | 3.4 | – |
| K | 1.6 | 1 | 2.4 | 5 | 2.9 | 3.4 | 1.2 | <1 | 2.6 | 2.7 | 2.6 | 2.7 |
| Na | <1 | – | 1.7 | – | <1 | 1.1 | <1 | – | 1.2 | 1.9 | 1.2 | 1.0 |

Specifically, it was found to be 9.4 wt % for sample I and 7.1 wt % for sample XII. The difference in the colors is most likely due to the significant difference in annealing temperatures [28].

It is of interest to compare the elemental compositions of the clay bases of Thasian amphorae: samples IV and V. The Si and Al contents in the samples are approximately the same and amount, respectively, to ~ 20 ± 2 and 9 ± 0.6 wt % (SEM/EDXS data) and 22± 4 and 11.5 ± 2 wt % (TEM/EDXS data). Na, K, Mg, Ca, and Fe cations, which are typical of clays, were also found in very close concentrations (with deviations within 1 wt %). An exception is the relatively low Ca content in sample IV in comparison with sample V: the difference is 3.2 wt %. The difference in the Ca contents for other samples (except for I) is larger. A comparison of the Bosporus tiles (samples I, XI and XII) exhibits a large distinction in the Si, Ca, and Fe contents. Thus, some characteristics of the elemental composition (specifically, the data on the clay base cation composition) coincide for the artifacts found in the same region.

*Results of Studying the Clay Base by the HRTEM and STEM/EDXS*

Additional studies of the clay base were performed for all samples by TEM/EDXS This method, in view of its higher locality, allows one to exclude the influence of relatively large microinclusions on the results obtained. The corresponding data are listed in Table 1. In most of all the samples under consideration STEM/EDXS, the Al and Si contents are somewhat higher as compared with the SEM/EDXS data. A surprising fact is the low Ca content in sample IV and a higher K content in sample V. The Fe content in the samples is also different. A comparison of the SEM/EDXS and STEM/EDXS data showed that the content of individual elements for the same sample may significantly differ, up to 9%. This is primarily related to the difference in the localities of the methods in use: 5–10 nm for STEM and 1–2 μm for SEM/EDXS. Thus, the regions analyzed by SEM/EDXS may contain inclusions, which affect the final elemental distribution. One cannot also exclude the influence of lattice orientation with respect to the

transmitted electron beam when STEM/EDXS is applied.

An analysis of the elemental distribution maps, obtained in a transmission electron microscope, showed that Ca, Fe, and Ti cations are generally concentrated in individual particles, in contrast to K, Na, and Mg cations, which are present usually in the aluminosilicate clay base.

An analysis of HRTEM micrographs, as shown in Fig. 3, revealed a number of periodicities, which correspond to interlayer spacings in argillaceous minerals (Table 2). Undoubtedly, these data were obtained from very small sample volumes; however, even based on them, one can draw preliminary conclusions on the nature of argillaceous minerals used in the production of artifacts. When analyzing structural parameters, one must take into account that the artifacts under study were heated to relatively high temperatures during fabrication. This heat treatment could lead to transformation or partial decomposition of argillaceous mineral. In particular, it was noted in [27] that the interlayer periodicity ceases to be observed in kaolinite and halloysite after their annealing at 600°C. At the same time, periodicities on the scale more than 1 nm are retained in illite, palygorskite, sepiolite, chlorite, and interstratified argillaceous minerals. Thus, palygorskite or interstratified argillaceous mineral could be used in sample I. Concerning samples II and VII, along with palygorskite or interstratified argillaceous minerals, one can suggest the presence of vermiculite or illite. Note that the discrepancy of the structural data for Thasian amphora samples IV and V may be due to the fact that they were fabricated at different times; this issue calls for further study, in particular, applying additional samples from the same region.

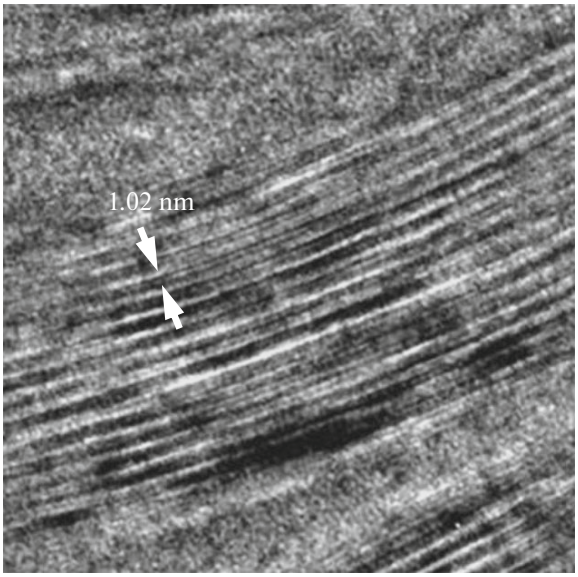


**Fig. 3.** HRTEM image of the clay base of a fragment of sample VII.

### *Study of Inclusions. OM Results in Comparison with SEM/EDXS Data*

Numerical estimates of the contents of inclusions of different color in the samples, based on the results of the OM study of laps, are listed in Table 3. The content of inclusions turned out to be maximum (25%) in the Colchian amphora (sample VII) and minimum (5%) in the Chios amphora (sample VIII). Returning to the OM data on "related" samples IV and V, one can conclude that they have different total contents of inclusions but a very close percentage of brown inclusions. The total contents of inclusions in the tiles from the same source (samples I and XI) coincide. An exception is the high total contents of inclusions in sample XII. However, the content of inclusions of the same type (specifically, of white color) is also approximately equal for samples I and XI: 6–7%.

In the second stage, we estimated the morphological features of the inclusions: color, shape, and faceting. Visually, the impurities vary in color from transparent milky white to black. As was noted above, the identification of inclusions of similar color and chemical composition may help to attribute products manufactured by a certain master. Their shape and size (in particular, irregular edges of relatively large inclusions) give grounds to suggest that these minerals were used as decorative elements; note also that they were mechanically ground before loading into the clay mass.

Black inclusions of two types were observed in the samples: (1) large (up to 1.2 mm in size) irregularly shaped inclusions, with a relatively high content of Ca and Mg (samples II, III, VI, VII, XII) and (2) smaller (about 0.2 mm in size) elliptical or spherical inclusions, with a high (according to the EDXS data) Fe content.

When describing inclusions, we took into account the EDXS/SEM data obtained from the sample regions presented in Fig. 2, as well as from other regions, which are omitted because of the limited volume of the paper. For example, Fig. 4 shows distribution maps of the main elements for sample VII. The

**Table 2.** Results of HRTEM analysis of the interplanar spacings in argillaceous minerals

| Sample | I | II | IV | VII | XII |
|---|---|---|---|---|---|
| Interplanar spacings, nm | 1.117 | 1.03, 1.06 | 1.53 | 0.99<br>1.02<br>1.04 | 1.02 |

For the samples that are absent in the table, no interlayer periodicities corresponding to any argillaceous minerals were found. This may be related to the specificity of preparing (grinding) samples for HRTEM or to a small volume analyzed.

**Table 3.** Estimated contents of inclusions, with indication of their color

| Sample<br>Inclination<br>color | I | II | III | IV | V | VI | VII | VIII | IX | X | XI | XII |
|---|---|---|---|---|---|---|---|---|---|---|---|---|
| Black | 1 | 12 | 4 | – | 7 | 5 | 14 | – | – | – | 4 | 3 |
| White | 6 | 2 | 2 | 5 | 3 | – | 11 | – | 6 | 1 | 7 | – |
| Brown | – | – | 3 | 8 | 6 | 2 | – | 5 | 6 | 11 | 2 | 4 |
| Total area | 7 | 14 | 9 | 13 | 16 | 7 | 25 | 5 | 12 | 12 | 13 | |

composition of the inclusions of each type was analyzed more thoroughly directly at a point from the inclusion region. The compositions of black and white inclusions are given in Tables 4 and 5, respectively.

Samples II, VI, VII, and XII have approximately the same content of Si, Ca, Fe, and Mg. The results of analyzing the elemental composition of inclusions in sample III are somewhat contradictory. An analysis of

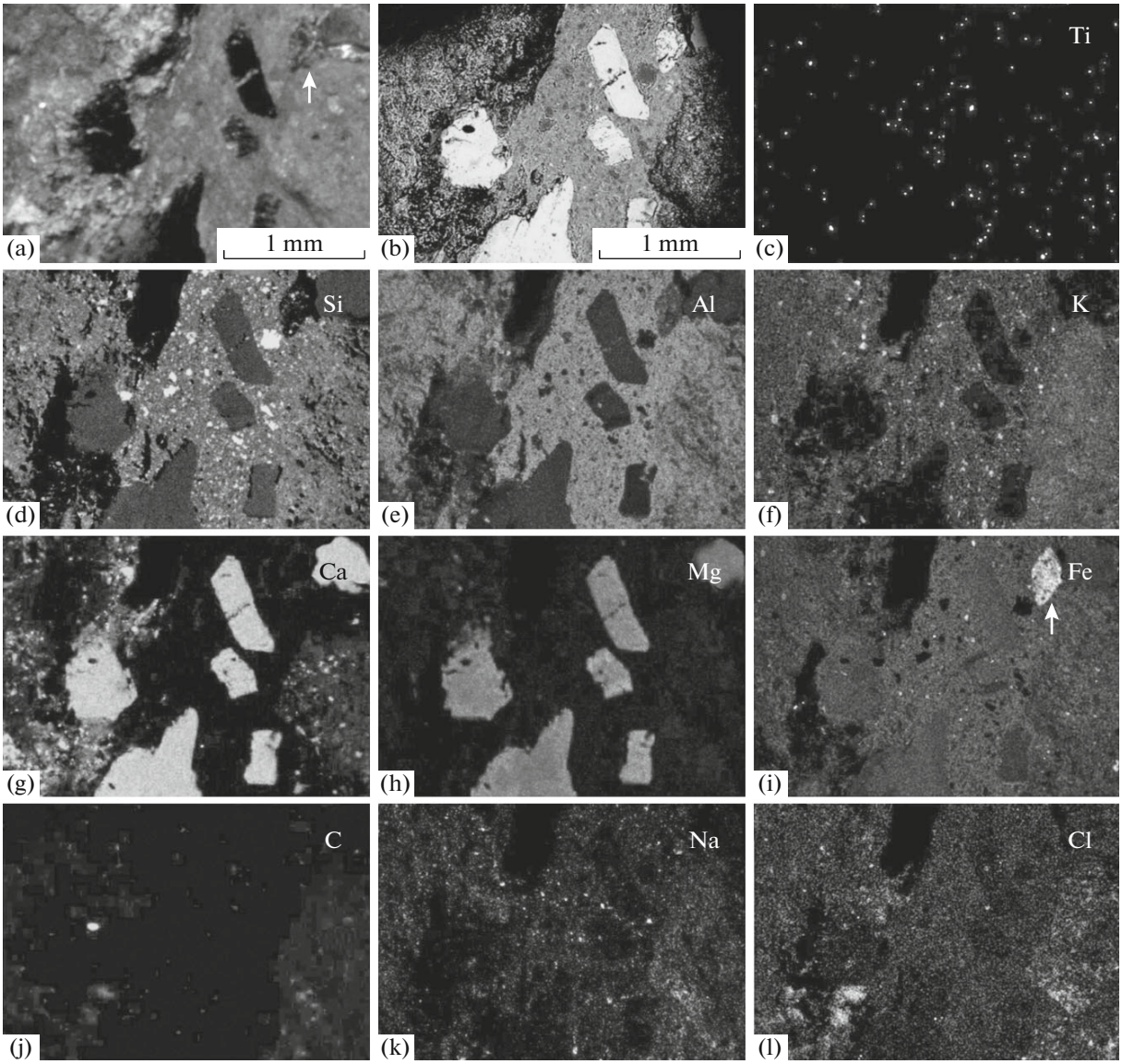


**Fig. 4.** Results of studying a lap of sample VII: (a) OM image, (b) SEM image in backscattered electrons; and (c–l) distribution maps of (c) Ti, (d) Si, (e) Al, (f) K, (g) Ca, (h) Mg, (i) Fe, (j) C, (k) Na, and (l) chlorine atoms.

**Table 4.** Comparative analysis of the composition of black inclusions

| Sample<br>Element | I | II | III-1 | III-2 | V-1 | V-2 | VI | VII | XI-1 | XI-2 | XII |
|---|---|---|---|---|---|---|---|---|---|---|---|
| O | 36.6 | 43.0 | 27.1 | 41.5 | 18.6 | 36.7 | 40.4 | 42.9 | 18.8 | 44.5 | 40.7 |
| Si | 12.1 | 23.0 | 3.4 | 19.3 | 7.8 | 17.9 | 20.2 | 21.9 | 12.5 | 21.4 | 20.4 |
| Ca | 1.9 | 16.4 | <1 | 8.3 | 3.4 | 2.2 | 17.0 | 16.9 | 4.0 | 5.7 | 15.9 |
| Al | 6.0 | 2.4 | 4.1 | 7.9 | 3.3 | 11.2 | 3.3 | 3.0 | 4.7 | 8.8 | 3.3 |
| Fe | 31.7 | 3.0 | 52.0 | 7.6 | 62.2 | 18.5 | 5.3 | 5.9 | 53.9 | 4.8 | 6.7 |
| Mg | 2.2 | 9.7 | 2.0 | 8.4 | <1 | 7.9 | 7.8 | 8.5 | 1.3 | 2.6 | 7.0 |
| C | 3.2 | 1.8 | 2.8 | 2.5 | 2.6 | 1.9 | 1.3 | – | 2.3 | 2.1 | 3.8 |
| K | 2.0 | <1 | <1 | 1.1 | <1 | 3.0 | <1 | – | <1 | 2.4 | <1 |
| Na | 2.1 | <1 | 1.6 | 2.2 | <1 | – | <1 | <1 | 1.5 | <1 | <1 |
| Ti | <1 | <1 | 6.4 | 1.2 | – | – | <1 | <1 | <1 | <1 | <1 |
| Cl | <1 | <1 | – | – | <1 | – | – | – | <1 | – | – |
| P | <1 | <1 | – | – | – | – | 3.3 | – | – | <1 | <1 |
| Mn | – | – | – | – | – | – | – | – | – | 4.6 | – |

**Table 5.** Comparative analysis of the composition of white inclusions

| Sample<br>Element | I | V | VII | XI | IV | IX | X |
|---|---|---|---|---|---|---|---|
| O | 42.7 | 40.7 | 54.3 | 46.2 | 44.7 | 47.1 | 53.6 |
| Si | 21.4 | 15.7 | 15.0 | 7.9 | 8.7 | 6.0 | 1.2 |
| Ca | 15.0 | 15.9 | 12.1 | 32.1 | 22.3 | 30.9 | 12.7 |
| Al | 5.8 | 3.3 | 2.9 | 3.1 | 4.6 | 2.1 | 3.9 |
| Fe | 4.1 | 4.2 | 2.4 | 2.9 | 2.7 | 1.3 | <1 |
| Mg | 1.2 | 1.2 | <1 | <1 | 1.6 | 1.9 | 1.8 |
| C | 6.3 | 16.0 | 10.1 | 6.4 | 6.5 | 7.4 | 15.9 |
| K | 1.5 | 1.6 | 1.2 | <1 | <1 | <1 | <1 |
| Na | <1 | <1 | <1 | <1 | 1.3 | 1.1 | 1.3 |
| Ti | <1 | <1 | <1 | – | – | – | – |
| Cl | <1 | <1 | <1 | <1 | 1.1 | <1 | <1 |
| P | <1 | <1 | <1 | <1 | <1 | <1 | <1 |
| S | <1 | <1 | <1 | <1 | <1 | <1 | 8.9 |
| F | – | – | – | – | 5.3 | – | – |

one group of inclusions (III-1) showed a low content of Si, Ca, and Mg but an extremely high Fe content. One can suggest iron to be present in the form of oxides. A similar pattern is observed in sample VII, where the selection shown by an arrow in the optical micrograph (Fig. 4a) contains a larger amount of iron (noted by an arrow in Fig. 4i). According to [5, 9, 22], iron oxides were often observed in the composition of ceramic products. The elemental composition of the second group (III-2) is similar to that of samples II,

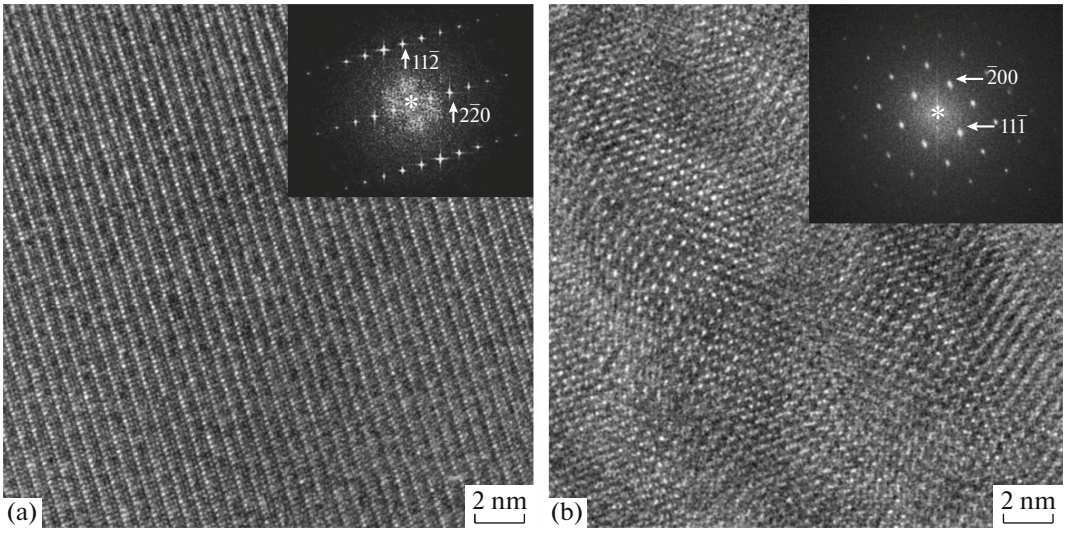


**Fig. 5.** HRTEM images of the augite lattice (sample VII, black inclusions), recorded with the (a) [111] and (b) [011] zone axes. The insets present numerical two-dimensional Fourier spectra.

VI, VII, and XII. Preliminary XRD data indicated that these samples may contain diopsides. It is not unbelievable that the same nonplastic material could be added to ceramic items produced in different pottery centers (samples II, VI, VII, and XII), because the minerals in use originate from a relatively similar geological environment, in which the ancient towns of the Black Sea Region were located.

A comparison of the composition of white inclusions based on the data of [5, 9, 22] suggests that they contain the following minerals: feldspar group, quartzes, and calcite. The first group includes representatives of solid solutions of the ternary system of the isomorphous series $K[AlSi_3O_8]$–$Na[AlSi_3O_8]$–$Ca[Al_2Si_2O_8]$, whose end terms are, respectively, orthoclase, albite, and anorthite. Inclusions may be isomorphic mixtures, for example, of anorthite ($CaAl_2Si_2O_8$) and albite ($NaAlSi_3O_8$). The results of our study suggest that the inclusions in samples I, V, and VII with a Si content more than 15 wt % are mixtures of spar-group minerals. The second group is most likely presented by calcites. An example is the inclusion in sample X with a high C content and a low Si content.

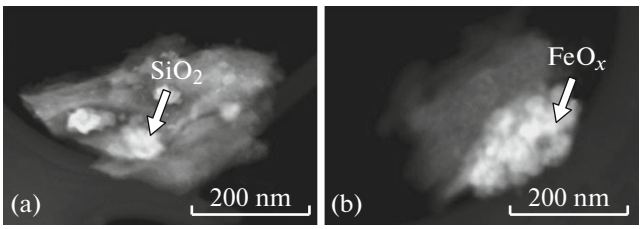


**Fig. 6.** Dark-field STEM images of small inclusions in the clay base: (a) $SiO_2$ and (b) $FeO_x$ particles.

A study of brown inclusions showed that their composition is close to that of white inclusions but with a much lower Ca content. These inclusions are likely also one of the feldspar species. At the same time, brown inclusions may be another type of nonplastic material, specifically, chamotte (ground burned ceramics).

### *Results of Studying Inclusions by the HRTEM and STEM/EDXS Methods*

As was noted above, minerals of black color, which turns dirty yellow here and there, were used as a nonplastic material in samples II, III, VI, VII, and XII. According to the preliminary XRD data, these minerals were characterized as diopsides from the pyroxene group. The study of black inclusions was continued by the TEM, ED, and STEM/EDXS methods on fragments cut from sample VII by an FIB. HRTEM images of these inclusions are presented in Fig. 5. The insets show two-dimensional Fourier spectra of these images. All data derived from the images and spectra indicate that the crystal structure with the sp. gr. $C2/c$ and the unit-cell parameters coincide with those of pyroxene-group minerals: diopside and augite; however, the STEM/EDXS data showed the Fe content in the samples to be 5–7 wt %. Therefore, the black inclusions under study are mineral augite in most cases [31].

An STEM/EDXS study of small inclusions in the clay base (on ground samples deposited on grids) showed the presence of iron oxide and silicon oxide inclusions. As an example, we present a dark-field STEM image of the inclusions found in the clay base of sample VII (Fig. 6). These are groups of particles

with a total size of 100–200 nm (however, some particles are less than 50 nm in size).

These inclusions are highly inhomogeneous, and their presence most likely affects the integral values of the elemental composition of artifacts.

## CONCLUSIONS

We reported the results of the first stage of the study aimed at compiling the general atlas of Crimean ceramics. The analysis of the ancient ceramics by microscopic methods with application of EDXS made it possible to conclude the following.

A comparison of the clay base color for the Thasian amphorae (i.e., the artifacts found in the same geographic region), samples IV and V, fabricated in III and IV BC, respectively, showed relatively similar colors and similar character of dispersivity. The Si and Al contents are approximately equal in all samples and amount to ~ 20 ± 2 and 9 ± 0.6 wt %, respectively (according to the SEM data), and 22 ± 4 and 11.5 ± 2 wt %, respectively (TEM data). Na, K, Mg, Ca, and Fe cations, which are typical of clays, were found in these samples in approximately equal concentrations, with deviations within 1 wt %. An exception is the relatively low Ca content in sample IV in comparison with sample V: the difference is 3.2 wt %.

The difference in the Si, Ca, and Fe contents in the clay base of Bosporus tiles (samples I, XI and XII) reaches 5, 2, and 1.7 wt %, respectively.

The difference in the HRTEM structural data on the clay base of Thasian amphorae can be explained by insufficient statistics and the difference in the annealing temperatures of these artifacts.

The content of different inclusions in related samples may either be similar or differ: according to the OM data, the percentage of brown inclusions in samples of Thasian amphorae is almost the same. White inclusions in Bosporus tiles (samples I and XI) were also found in equal concentrations: 6–7%.

The suggested nonplastic materials in samples II, III, VI, VII, and XII are mainly relatively large augite inclusions.

Along with augite, inclusions of feldspar, iron oxides, and silicon oxides were also found in the samples.

Thereafter the proposed approach will be used when studying other archaeological ceramic artifacts (found in other RF regions and dated to other time periods): the physicochemical characteristics of ceramic artifacts produced in known centers will be used as reference data for establishing the production sites of ceramic materials whose origin is unknown.

## ACKNOWLEDGMENTS

This study was supported by the Russian Foundation for Basic Research, project no. 17-29-04201, in the part of electron microscopy studies and the Federal Agency for Scientific Organizations (contract no. 007-ГЗ/Ч3363/26) in the part of X-ray diffraction tests on the synchrotron radiation source "Kurchatov" at the National Research Centre "Kurchatov Institute."

## REFERENCES

1. P. M. Rice, *Pottery Analysis* (Univ. of Chicago Press, Chicago, 2015).
2. *Analytical Archaeometry. Selected Topics,* Ed. by G. M. Howell (RSC, Cambridge, 2012).
3. P. Dilmann, L. Bellot-Gurlet, and I. Nenner, *Nanoscience and Cultural Heritage* (Atlantic Press, New York, 2016).
4. The Oxford Handbook of Archaeological Ceramic Analysis, Ed. by A. Hunt (Oxford Univ. Press, Oxford, 2017).
5. M. Emami, Y. Sakalib, C. Pritzel, and R. Trettin, J. Microsc. Ultrastruct. **4**, 11 (2016).
6. J. Ross, K. D. Fowler, I. Shai, et al., J. Archeol. Sci. Rep. **18**, 551 (2018).
7. Z. L. Epossi Ntah, R. Sobott, B. Fabbri, and K. Bente, Cerâmica **63**, 413 (2017).
8. T. I. Teterina, Vestn. Ross. Akad. Nauk, No. **2**, 13 (2012).
9. H. V. Cabadas-Báez, B. Solís-Castillo, E. Solleiro-Rebolledo, et al., Geoarchaeology **32**, 382 (2017).
10. I. B. Brashinskii, *Methods for Studying the Ancient Trade (by an Example of Northern Black Sea Region),* Ed. by A. N. Shcheglov (Nauka, Leningrad, 1984) [in Russian].
11. A. N. Shcheglov and N. B. Selivanova, *Greek Amphorae: Problems of the Development of Handicrafts and Trade in the Ancient World* (Izd-vo Saratov Univ., Saratov, 1992) [in Russian], p. 32.
12. S. Yu. Vnukov, *Amphorae from the Black Sea Region, Dated to the I BC–II AD.* Part II: *Petrography, Chronology, Problems of Trade* (Aleteia, St. Petersburg, 2006) [in Russian].
13. *Physical and Chemical Study of Ceramics (on the Example of the Transition-Time Items from the Bronze to Iron Age,* Ed. by V. V. Boldyrev and V. I. Molodin (Izd-vo SO RAN, Novosibirsk, 2006) [in Russian].
14. I. K. Whitbread, *Greek Transport Amphorae. A Petrological and Archaeological Study. British School at Athens, Fitch Laboratory Occasional Paper 4. xxiv+453 p.* (The British School at Athens, Athens, 1995).
15. M. Kibaroğlu, M. Satır, and G. Kastl, J. Archaeol. Sci. **36**, 2463 (2009).
16. Yu. K. Guguev, V. Yu. Malashev, and V. G. Rylov, Nizhnevolzhskii Arkheol. Vestn. **16** (1), 45 (2017).

17. M. Kulkova and A. Kulkov, The Old Potter's Almanach **21** (1), 2 (2016).
18. M. A. Kulkova, T. M. Gusentsova, T. V. Sapelko, et al., J. Mar. Syst. **129**, 19 (2014).
19. M. A. Kulkova and A. M. Kulkov, Microsc. Anal. **136**, 7 (2015).
20. A. L. Vasil'ev, M. V. Koval'chuk, and E. B. Yatsishina, Crystallogr. Rep. **61** (6), 873 (2016).
21. E. Doehne and D. C. Stulik, Scanning Microsc. **4** (2), 275 (1990).
22. C. Knappett, D. Pirrie, M. R. Poweret, et al., J. Archaeol. Sci. **38**, 319 (2010).
23. T. A. Khoroshun and I. M. Summanen, Tr. Karel'skogo Nauch. Tsentra Ross. Akad. Nauk, No. **8**, 17 (2015).
24. E. Badea, L. Miu, P. Budrugeac, et al., J. Therm. Anal. Calorim. **91** (1), 17 (2008).
25. D. B. Harden and J. M. C. Toynbee, Archaeologia **97**, 179 (1959).
26. N. N. Kolobylina, E. A. Greshnikov, A. L. Vasil'ev, et al., Crystallogr. Rep. **62** (4), 543 (2017).
27. V. I. Osipov and V. N. Sokolov, *Clays and Their Properties* (Geos, Moscow, 2013) [in Russian].
28. Yu. B. Tsetlin, Vopr. Arkheol. Povolzh'ya, No. **4**, 421 (2006).
29. L. Bindi, O. G. Safonov, V. O. Yapaskurt, et al., Am. Mineral. **88**, 464 (2003).

*Translated by Yu. Sin'kov*